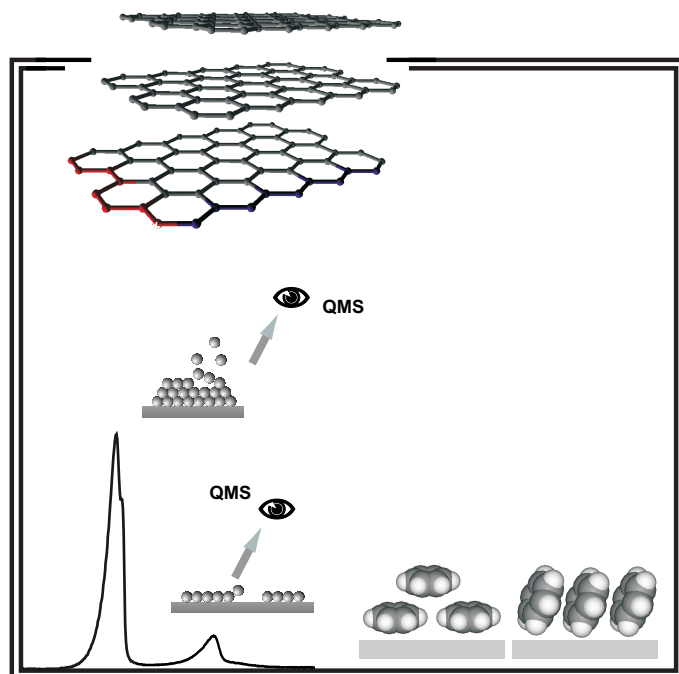


# **Desorption of gases from graphitic and porous carbon surfaces**



**Dissertation**  
zur Erlangung des akademischen Grades  
**doctor rerum naturalium**  
im Fachbereich Chemie der Freien Universität Berlin  
eingereichte Dissertation  
von  
**M.Sc. Renju Zacharia**  
aus Kottayam, Indien



# **Desorption of gases from graphitic and porous carbon surfaces**

**Dissertation**

zur Erlangung des akademischen Grades

**doctor rerum naturalium**

(Dr. rer. nat.)

im Fachbereich Chemie  
der Freien Universität Berlin  
eingereichte Dissertation

von

**M.Sc. Renju Zacharia**  
aus Kottayam, Indien

May 2004  
Berlin



Die vorliegende Arbeit wurde in der Zeit von April 2001 bis März 2004 am Fritz-Haber-Institut der Max-Planck-Gesellschaft in Berlin unter der Leitung von Prof. Dr. G. Ertl angefertigt.

Gutachter

1. Prof. Dr. G. Ertl
2. Prof. Dr. R. Schlögl

Datum der Disputation: 09 June 2004



# Contents

<b>1 Introduction</b>	<b>1</b>
<b>2 Concepts</b>	<b>5</b>
2.1 Physisorption . . . . .	6
2.1.1 Energetics of physisorption . . . . .	6
2.1.2 Desorption of physisorbed species . . . . .	8
2.1.3 Desorption from porous carbon surfaces . . . . .	10
2.2 Chemisorption . . . . .	11
2.2.1 Energetics of chemisorption . . . . .	12
2.2.2 Chemisorption in heterogeneous catalysis . . . . .	14
<b>3 Materials and methods</b>	<b>17</b>
3.1 Experimental setup . . . . .	18
3.1.1 UHV chamber and vacuum system . . . . .	18
3.1.2 Sample holder . . . . .	19
3.1.3 Gas dosing system . . . . .	20
3.1.4 Temperature measurement and control . . . . .	21
3.1.5 Pressure and desorption rate measurement . . . . .	21
3.1.6 Data acquisition . . . . .	22
3.2 Sample preparation . . . . .	22
3.2.1 Graphite . . . . .	22
3.2.2 Single-wall carbon nanotube bundles . . . . .	23
3.2.3 Carbon nanofibers . . . . .	25
3.2.4 Colloidal graphite . . . . .	27
3.3 Temperature programmed desorption . . . . .	27
3.3.1 Principles . . . . .	27
3.3.2 Temperature programmed oxidation . . . . .	29
3.3.3 Analysis of TDS data . . . . .	29
<b>4 Energetics of interlayer binding in graphite</b>	<b>35</b>
4.1 Graphite: Structure and properties . . . . .	36
4.1.1 Lattice structure . . . . .	37

4.1.2	Interlayer cohesive energy of graphite . . . . .	38
4.1.3	Polyaromatic hydrocarbons on graphite: The model system . .	41
4.2	Desorption kinetics of polyaromatic hydrocarbons . . . . .	42
4.2.1	Temperature programmed desorption of PAHs . . . . .	43
4.2.2	Determination of frequency factors and binding energies . .	48
4.2.3	Dependence of PAH binding energies on static polarizabilities	53
4.3	Interlayer cohesive energy of graphite . . . . .	56
4.3.1	Determination of carbon-carbon interaction potential . . . .	56
4.4	Summary and outlook . . . . .	59
<b>5</b>	<b>Oxidation of graphitic surfaces</b>	<b>61</b>
5.1	Physisorption of oxygen . . . . .	63
5.2	Chemisorption of oxygen . . . . .	63
5.2.1	Mechanism of graphite oxidation . . . . .	64
5.2.2	Carbon-oxygen surface functional groups . . . . .	66
5.3	Temperature programmed oxidation of carbon surfaces . . . .	68
5.3.1	Thermal desorption of hydrogen peroxide . . . . .	68
5.3.2	Decarbonylation and decarboxylation of carbon surfaces . .	74
5.4	Summary and outlook . . . . .	76
<b>6</b>	<b>Oxidative dehydrogenation on carbon surfaces</b>	<b>79</b>
6.1	Carbon in heterogeneous catalysis . . . . .	80
6.1.1	Oxidative dehydrogenation on carbon surfaces . . . . .	80
6.1.2	Mechanism of oxidative dehydrogenation of ethylbenzene . .	82
6.2	Desorption kinetics of ethylbenzene from carbon surfaces . . .	85
6.2.1	Temperature programmed desorption from carbon surfaces .	86
6.2.2	Activation energy and pre-exponential factors . . . . .	91
6.3	Desorption kinetics of ethylbenzene from oxidized carbon surfaces . .	93
6.3.1	Temperature programmed desorption from oxidized carbon surfaces . . . . .	94
6.3.2	Analysis of catalytic activity of carbon substrates . . . . .	100
6.4	Summary and outlook . . . . .	103
<b>7</b>	<b>Conclusions</b>	<b>105</b>
<b>A – Vapor pressure curves</b>		<b>109</b>
<b>B – Instruments</b>		<b>111</b>
B.1	UHV system . . . . .	111
B.2	Sample preparation . . . . .	112
B.3	Data acquisition . . . . .	112

<b>References</b>	<b>113</b>
<b>Kurzfassung</b>	<b>125</b>
<b>Abstract</b>	<b>127</b>
<b>Publications</b>	<b>129</b>
<b>Acknowledgments</b>	<b>131</b>
<b>Curriculum Vita</b>	<b>133</b>



# List of Figures

2.1	Schematic illustration of image states when an atom approaches a solid surface . . . . .	6
2.2	Potential energy diagram corresponding to physisorption of neutral atoms or molecules on solid surfaces . . . . .	7
2.3	Schematic representation of the three growth modes during physisorption at different coverage regimes . . . . .	9
2.4	Schematic representation of surface diffusion and desorption from a porous structure . . . . .	11
2.5	The potential energy diagram corresponding to the dissociative chemisorption of a neutral diatomic molecule on a solid surface . . . . .	13
2.6	Schematic illustration of the elementary process in heterogeneous catalysis . . . . .	15
3.1	Schematic illustration of the UHV chamber and other accessories used in the experiments . . . . .	18
3.2	Photograph of all parts in the sample holder assembly . . . . .	19
3.3	Illustration of the structural relation between single-wall carbon nanotubes and graphene sheet . . . . .	24
3.4	Microscopic features of the bucky paper . . . . .	25
3.5	Schematic illustration and TEM image of carbon nanofibers . . . . .	26
3.6	Illustration of processes during dosing and temperature programmed desorption experiment . . . . .	28
3.7	Thermal desorption spectrum of ethylbenzene from the surface of highly oriented pyrolytic graphite . . . . .	31
3.8	Illustration of the Falconer-Madix method of analysis of TD spectra .	32
3.9	Illustration of the analysis of isotherms and intercept plots from the Falconer-Madix method . . . . .	33
4.1	Crystal structure of hexagonal graphite . . . . .	37
4.2	$\pi$ -bonding and anti-bonding wave functions from the first Brillouin zone of graphene. . . . .	38
4.3	Three-dimensional Brillouin zone of graphite . . . . .	39

4.4	Commensurate monolayer (ML) structure of coronene on graphite surface . . . . .	41
4.5	Series of thermal desorption spectra of benzene from HOPG surface . . . . .	43
4.6	Desorption features of benzene from graphite surface in the sub-monolayer region . . . . .	44
4.7	Schematic illustration of coverage dependent configurations of benzene molecules on graphite surface . . . . .	45
4.8	Series of thermal desorption spectra of naphthalene from HOPG surface . . . . .	46
4.9	Series of thermal desorption spectra of coronene from HOPG . . . . .	47
4.10	Series of thermal desorption spectra of ovalene desorption from graphite surface . . . . .	47
4.11	Extrapolation of benzene vapor pressure data to the desorption temperature using Antoine's fit function . . . . .	50
4.12	Isothermal desorption plots for benzene desorption from HOPG . . . . .	52
4.13	Intercept plot of benzene desorption from HOPG obtained from the fit to desorption isotherms . . . . .	53
4.14	Activation energies of PAH desorption from graphite surface as a function of PAH molecular static polarizability . . . . .	55
4.15	Dependence of activation energy for polyaromatic hydrocarbon desorption on the number of carbon atoms from four PAHs . . . . .	58
5.1	Schematic illustration of basal and edge planes in graphitic lattice . . . . .	65
5.2	Relative stability of various activated oxygen species in the gas phase, on the surface, and within the lattice . . . . .	66
5.3	Polyfunctional organic groups formed on carbon surfaces as a result of the oxidation . . . . .	67
5.4	Series of TD spectra of molecular oxygen desorption from carbon nanofibers . . . . .	70
5.5	Thermal desorption spectra of SF <sub>6</sub> from carbon nanofibers prior to and after oxidation . . . . .	71
5.6	Series of thermal desorption spectra of oxygen desorbing from colloidal graphite . . . . .	72
5.7	Intercept plot for desorption isotherms of oxygen from colloidal graphite surface . . . . .	72
5.8	Illustration of the ER mechanism between molecular oxygen and an armchair edge of a graphene sheet . . . . .	73
5.9	Thermal desorption spectra of (a) CO, (b) CO <sub>2</sub> and (c) oxygen after exposing carbon nanofibers with hydrogen peroxide . . . . .	75
5.10	Thermal desorption spectra of (a) CO (b) CO <sub>2</sub> and (c) oxygen after exposing colloidal graphite with hydrogen peroxide . . . . .	76

---

6.1	TEM image of graphitic deposit formed over K-promoted Fe <sub>2</sub> O <sub>3</sub> during ethylbenzene ODH . . . . .	81
6.2	Schematic representation of elementary processes under Langmuir-Hinshelwood mechanism . . . . .	84
6.3	Series of thermal desorption spectra of ethylbenzene from HOPG . . . . .	86
6.4	Series of thermal desorption spectra of ethylbenzene from SWNT bundles . . . . .	87
6.5	Schematic representation of surface diffusion and desorption from a porous structure . . . . .	88
6.6	Series of high coverage thermal desorption spectra of ethylbenzene from SWNT bundles . . . . .	89
6.7	Series of thermal desorption spectra of ethylbenzene from carbon nanofibers . . . . .	89
6.8	Series of thermal desorption spectra of ethylbenzene from colloidal graphite surface . . . . .	90
6.9	Isotherms constructed from the thermal desorption of ethylbenzene from HOPG . . . . .	91
6.10	Intercept plots for the ethylbenzene desorption from HOPG, nanotubes, nanofibers and colloidal graphite . . . . .	92
6.11	Schematic representation of edge and basal planes of a graphitic substrate . . . . .	94
6.12	Mass spectra of ethylbenzene and styrene showing peaks corresponding to different fragments . . . . .	95
6.13	Series of thermal desorption spectra of ethylbenzene and styrene desorption from oxidized carbon nanofibers . . . . .	96
6.14	Series of thermal desorption spectra of ethylbenzene and styrene desorption from oxidized carbon colloidal graphite . . . . .	97
6.15	Intercept plots for the desorption of ethylbenzene and styrene from oxidized carbon nanofibers . . . . .	97
6.16	Chemisorption of oxygen on an armchair edge of graphene sheet and formation of quinone surface functional group . . . . .	98
6.17	Reaction mechanism for the ethylbenzene oxidative dehydrogenation analogous to that in classical organic chemistry . . . . .	99
6.18	Resonance stabilization of the ethylbenzene carbocation formed during the oxidative dehydrogenation reaction . . . . .	99
6.19	Surface concentration of ethylbenzene on colloidal graphite as a function of temperature . . . . .	101
6.20	Surface concentration of styrene on colloidal graphite as a function of temperature . . . . .	101
6.21	Selectivity to form styrene on carbon nanofibers and colloidal graphite surfaces as a function of surface temperature . . . . .	102

---

A.1 Temperature dependence of vapor pressure of (a) benzene (b) naphthalene and (c) coronene and Antoine's extrapolation . . . . .	110
--	-----

# List of Tables

4.1	Interlayer cohesive energy of graphite calculated by various theoretical and experimental methods . . . . .	40
4.2	Molecular structure and properties of polycyclic aromatic hydrocarbons . . . . .	42
4.3	Antoine's fit parameters, vapor pressure data and molecular static polarizabilities of benzene, naphthalene, coronene and ovalene . . . . .	51
4.4	Activation energies and pre-exponential frequency factors of polycyclic aromatic hydrocarbon desorption from graphite . . . . .	51
5.1	Decarbonylation and decarboxylation reactions from the classical organic chemistry . . . . .	67
6.1	Activation energies and pre-exponential frequency factors for ethylbenzene desorption from graphite, nanotubes, nanofibers and colloidal graphite . . . . .	93
6.2	Activation energies and pre-exponential frequency factors for ethylbenzene and styrene desorption from oxidized carbon nanofibers and colloidal graphite . . . . .	98
A.1	Antoine's fit parameters for the extrapolation of PAH vapor pressure	109



# Abbreviations and acronyms

CDD	<i>Coupled desorption diffusion</i>
CNF	<i>Carbon nanofiber</i>
CNT	<i>Carbon nanotube</i>
DFT	<i>Density functional theory</i>
ER	<i>Eley-Rideal Mechanism</i>
FM	<i>Falconer-Madix method</i>
HOPG	<i>Highly oriented pyrolytic graphite</i>
LH	<i>Langmuir-Hinshelwood mechanism</i>
LEED	<i>Low energy electron diffraction</i>
MvK	<i>Mars-van Krevelen mechanism</i>
MM3	<i>Molecular mechanics force field 3</i>
MWNT	<i>Multi-wall carbon nanotube</i>
ML	<i>Monolayer</i>
ODH	<i>Oxidative dehydrogenation</i>
PAH	<i>Polyaromatic hydrocarbon</i>
QMS	<i>Quadrupole mass spectrometer</i>
STM	<i>Scanning tunnelling microscopy</i>
SWNT	<i>Single-wall carbon nanotube</i>
TEM	<i>Transmission electron microscopy</i>
TD	<i>Thermal desorption</i>
TDS	<i>Thermal desorption spectroscopy</i>
TPD	<i>Temperature programmed desorption</i>
TST	<i>Transition state theory</i>
UHV	<i>Ultrahigh vacuum</i>
vdW	<i>van der Waals</i>



# List of Symbols

$\alpha$	<i>molecular static polarizability</i>	$\text{\AA}^3$
$\alpha_{zz}$	<i>z-component of polarizability tensor</i>	$\text{\AA}^3$
$\beta$	<i>heating rate</i>	$\text{K s}^{-1}$
$\nu$	<i>frequency factor</i>	$\text{s}^{-1}$
$\sigma$	<i>number of adsorbates per unit area</i>	$\text{m}^{-2}$
$\theta$	<i>surface coverage</i>	ML
$[A]_g$	<i>gas phase concentration of adsorbate A</i>	$\text{mol m}^{-3}$
$[A]_s$	<i>surface concentration of adsorbate A</i>	$\text{mol m}^{-2}$
$C_{EB}$	<i>percentage conversion of ethylbenzene</i>	-
$E_b$	<i>binding energy</i>	eV
$E_{cl}$	<i>cleavage energy of graphite</i>	eV
$E_d$	<i>activation energy of desorption</i>	eV
$k_i$	<i>rate constant</i>	$\text{mol m}^{-3} \text{ s}^{-1}$
$k_B$	<i>Boltzmann constant</i>	$\text{J K}^{-1}$
$m$	<i>molecular mass</i>	kg
$n$	<i>order of desorption</i>	-
$s, s_0$	<i>sticking coefficient</i>	-
$S_{ST}$	<i>selectivity to form styrene</i>	-
$T, T_0, T_{max}$	<i>temperature</i>	K
$p, p_0$	<i>pressure</i>	mbar
$V_{vdW}$	<i>van der Waals potential</i>	eV

